Journal of the Korean Physical Society, Vol. 47, No. 2, August 2005, pp. 277∼282

Structural and Electrical Analysis of Silicon Thin Films Deposited by Transformer-Coupled-Plasma Chemical-Vapor Deposition

Hyoung Cheol Lee* and Geun Young Yeom
Department of Materials Engineering, Sungkyunkwan University, Suwon 440-746

Yoo Jin Lee and Jin Koog Shin
Nano Information & Energy Storage Center, Korean Electronics Technology Institute(KETI), Seongnam 463-816

Sung Il Baik and Young Woon Kim
Department of Materials Engineering, Seoul National University, Seoul 151-742

(Received 1 April 2005)

In this study, silicon thin films were deposited by using a transformer-coupled-plasma chemical-vapor deposition (TCPCVD) technique using $SiH_4/H_2/PH_3$, and the effects of rf power on the structural and the electrical properties of the deposited thin films were investigated for applications to silicon solar cells. Increasing the rf power from 50 to 500 W increased the percent of crystalline silicon in the film from 42 to about 79 %. The increase in crystalline silicon was mostly attributed to an increase in the number of nanosized crystalline silicon grains having grain sizes from 3 to 15 nm. The increase in crystalline percent was also accompanied by an increase in the stress in the film. The increased crystalline silicon percent in the films increased the dark conductivity and, at 500 W of rf power, a dark conductivity of 10 $\Omega^{-1}\text{cm}^{-1}$ could be obtained for a 40-nm-thick film, which is applicable to silicon-based solar cells.

PACS numbers: 73
Keywords: Transformer-coupled-plasma chemical-vapor deposition, Microcrystalline, Rf power, Grain size, Solar cell

I. INTRODUCTION

Hydrogenated nano/microcrystalline silicon (c-Si : H), as well as hydrogenated amorphous silicon (a-Si : H), has been recognized as a useful thin-film semiconductor material for optoelectronic and electronic device applications, such as solar cells, thin film transistors, *etc.* [1,2]. In particular, highly phosphorous-doped n-type c-Si:H is very attractive in large-area electronics due to its much higher conductivity, higher doping efficiency, and lower optical absorption coefficient in the visible region (300-600 nm) compared to its amorphous counterpart [3].

The deposition of c-Si : H has been carried out by using various methods, such as hot-wire chemical-vapor deposition (HWCVD) [4, 5], photo-chemical vapor deposition (P-CVD) [6], plasma-enhanced chemical-vapor deposition (PECVD) using an electron cyclotron resonance (ECR) plasma [7], *etc.* Among these various methods, PECVD utilizing various plasmas, such as a capacitively coupled plasma [8], an ECR plasma, an inductively coupled plasma (ICP), *etc.* has been used as the most general deposition method for the deposition of hydrogenated microcrystalline silicon (μc-Si : H) [9]. The electrical, structural, and optical properties of n-type microcrystalline silicon deposited by using high density PECVD depend on the various deposition parameters, such as the ratio of hydrogen dilution, the concentrations of the dopants, the deposition temperature, the radio frequency (rf) power, *etc.* [10]. The deposition parameters change the nucleation and the growth characteristics of the film, such as the evolution of a long-range order microcrystals, and finally, they change the electrical and the structural properties [11].

In this study, phosphorous-doped hydrogenated silicon films were deposited at 300 °C on glass substrates by using a transformer-coupled plasma (TCP), which is a modified type of ICP for applications to solar cells, and where c-Si : H having a high electrical conductivity and low light-induced degradation must be achieved by depositing hydrogenated silicon with a low defect density. By varying the rf power of the TCP, we studied the

*E-mail: hclee@skku.edu

growth characteristics of c-Si : H can and investigated the relation between the structural properties of c-Si : H and its electrical properties in order to obtain n-type c-Si : H with a low defect density applicable to solar cells.

II. EXPERIMENT

Fig. 1 shows the transformer-coupled-plasma chemi cal-vapor deposition (TCPCVD) system operated at 13.56 MHz to grow n-type c-Si : H. Corning 1737 glass samples or 400-nm-thick grown SiO_2 silicon wafers were loaded and unloaded through the robot loadlock chamber to keep the process chamber at vacuum. The base pressure of the process chamber was kept lower than 8 $\times$ 10^{-7} Torr. The distance between the dielectric of the TCP electrode and the substrate holder was 4 cm. The diameter of the substrate holder was 100 mm and the substrate was heated to 300 °C for the deposition of c-Si : H. To deposit c-Si : H, we fed a gas on composed of SiH_4 (silane), H_2 (hydrogen), PH_3 (phosphine) from the top of the chamber, as shown in Fig. 1. The ratio of PH_3/SiH_4 was kept at 0.16, and the ratio of $H_2/(H_2 + PH_3 + SiH_4)$ was kept at 0.985. The total gas flow rate was maintained at 200 sccm, and the operational pressure was kept at 200 mTorr. The rf power was varied from 50 to 500 W to study the effect of the rf power on the characteristics of the deposited hydrogenated silicon thin film.

The radicals dissociated during the operation of the TCP were observed using optical emission spectroscopy (OES, PCM 420 SC Technology). The crystallinity of the deposited hydrogenated silicon thin film was investigated by using micro-Raman spectroscopy (Invia Basic Renisaw) with a 510-nm Ar^+ laser. The crystal orientation and the grain size of the deposited microcrystalline silicon were investigated by using a high-resolution X-ray diffraction (HRXRD, D8 Discover Bruker) with Cu $K\alpha_1$ (1.54 Å). The microstructure of the deposited hydrogenated silicon thin film was observed using high-resolution transmission electron microscopy (HRTEM, JEOL JEM 3000F). The dark conductivity was calculated by using the I-V characteristics of the films after the formation of two Aluminum ohmic contacts by thermal evaporation, as suggested by Concari *et al.* [12].

III. RESULTS AND DISSCUSSION

Fig. 2 shows the Raman spectra of the c-Si : H thin films deposited at various rf powers. In general, the hydrogenated silicon thin film consists of a-Si : H and c-Si : H, and the c-Si : H is composed of non-strained crystalline (single-crystalline) silicon and strained crystalline (or grain-boundary-like, nano/micro) silicon [7]. The Raman peaks of the a-Si : H, the strained c-Si : H, and the non-strained c-Si : H are located at 480 cm^{-1}, 508 $\sim$ 515 cm^{-1}, and 520 cm^{-1} respectively [13–15]. Due to the mixture of the three peaks, the Raman peak related to the silicon appears as a merged peak, as shown in Fig. 2. Especially, when the rf power was lower than 200 W, the peaks related to the crystalline Si are low; therefore, the Raman peak is broad. However, when the rf power is higher than 200 W, due to a decrease in the amount of amorphous silicon at 480 cm^{-1} and an increase in the amount of crystalline silicon, especially at 508 $\sim$ 515 cm^{-1}, sharper Raman peaks are observed.

Also, as Fig. 2 shows, when the rf power is increased, the peak related to the strained c-Si : H located at 508 $\sim$ 515 cm^{-1} has a relative shift from around 514 cm^{-1} at 200 W to 508 cm^{-1} at 500 W. The shift in the Raman peak related to the non-strained c-Si : H appears to be from the stress in the growing nano/micron-sized crystals. In fact, the shift in the Raman peak located around 508 $\sim$ 515 cm^{-1} has been observed by many re-

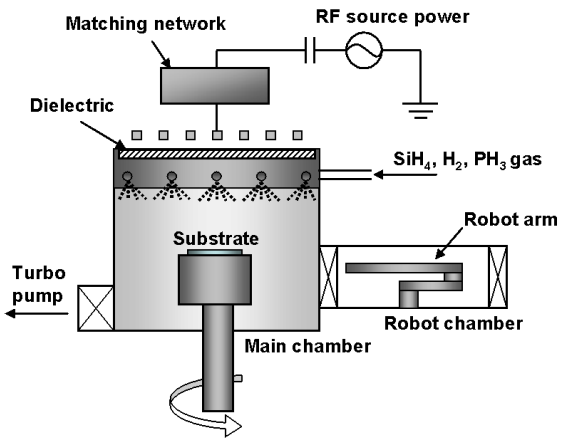

Fig. 1. Schematic diagram of the TCPCVD system used to deposit hydrogenated silicon films in this study.

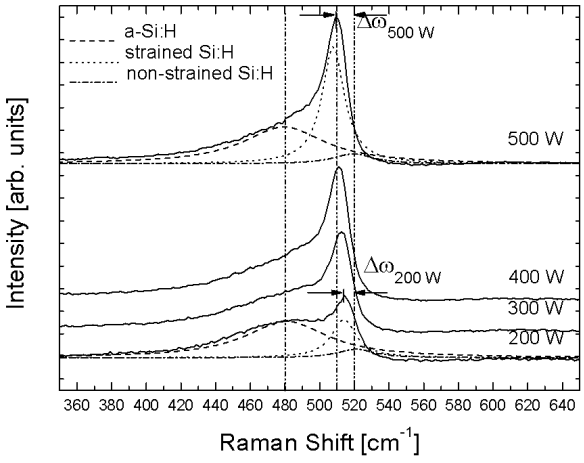

Fig. 2. Raman spectra of the hydrogenated silicon films deposited at various of rf source powers.

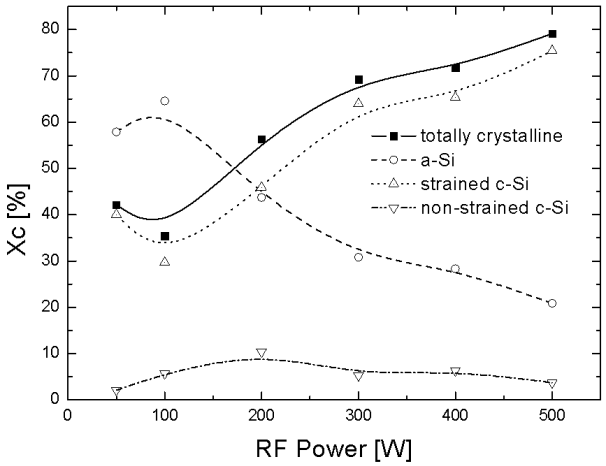

Fig. 3. Volume percentages (X_c) of a-Si : H, strained c-Si : H, non-strained c-Si : H, and totally crystalline silicon of the deposited hydrogenated silicon thin films as a function of the rf power from 50 to 500 W.

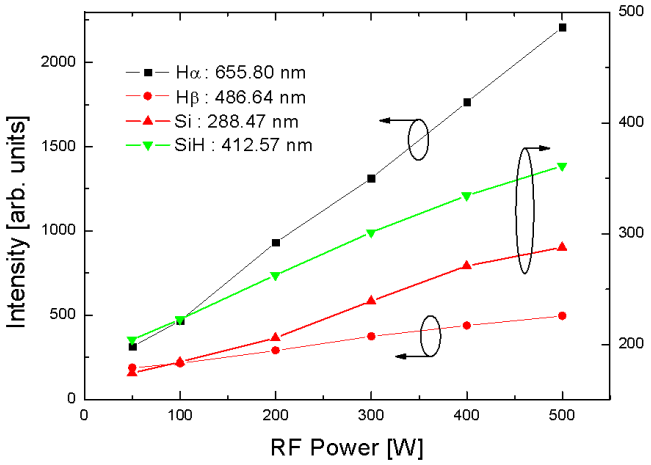

Fig. 4. Optical emission spectra of dissociated species, such as H, Si, and SiH, in the plasma as a function of the rf power from 50 to 500 W for a gas mixture composed of SiH_4, H_2, and PH_3.

searchers [13–15] and has been explained as being due to a change of strain in the lattice of the crystal. As the number of the nano/micro-crystalline grains in the film and the percent of cystallinity of the film increase with increasing rf power, the percent of grain boundaries in the film increases, and microcrystalline grains having different crystal orientations get closer to each other. In fact, the Raman peak of strained c-Si : H, I_g , near 508 $\sim$ 515 cm^{-1} is related to the grain boundary of the nano/micro-crystalline grains, and as the nano/micro-crystalline grains get closer and closer, the Raman peak appears to change due to an increase in the stress between nano/micron-sized crystalline grains having different crystal orientations.

The increase in the crystallinity with increasing rf power can be shown by the deconvolution of the Raman peaks to three peaks, a-Si : H, strained c-Si : H, and non-strained c-Si : H, by using a Lorentzian curve fitting [16]. Fig. 3 shows the percents of a-Si : H, strained c-Si : H, and non-strained c-Si : H in the deposited film as a function of the rf power. For the figure, the total crystalline silicon percent (X_c), which includes strained and non-strained crystalline silicon, was calculated as follows:

$$X_c = \frac{I_g + I_c}{I_g + I_c + \eta I_a} \times 100\ \% \qquad (1)$$

where I_c is the deconvoluted Raman peak intensity at 520 cm^{-1} from the non-strained c-Si : H, I_g is the intensity at 508 $\sim$ 515 cm^{-1} from the strained c-Si : H, and I_a is the intensity at 480 cm^{-1} from the a-Si : H. $\eta \approx 1.0$ is the ratio of the integrated Raman cross-section for crystalline silicon to that for amorphous silicon [17]. As figure shows, with increasing rf power from 50 W (about 100 nm in thickness) to 500 W (540 nm in thickness), the amorphous silicon percent decreases from about 57 % to 21 % while the strained c-Si : H percent increases from 40 % to 75 %. In the case of non-strained c-Si : H, the percent does not vary significantly with increasing rf power and remains at an within average of 5.6 %. The total crystalline percentage increased from 42 % at 50 W to 79 % at 500 W. The increase in the strained c-Si : H percent in the film with increasing rf power without any significant change in the percent of non-strained c-Si : H appears to show an increase in the number of nano/micro-crystalline silicon grains rather than a growth of existing grains.

The increase in the crystalline percent with increasing rf power appears related to an increase in ionization and dissociation from SiH_4 and H_2. Matsuda [18] and Sriraman *et al.* [19] showed that an increase of SiH_3 and H in the plasma played an important role in increasing the crystallization of deposited silicon films. An increase of the ion density will also increase the crystallization of the deposited film, as suggested by H. Yang *et al.* [20]. Using OES, the radical species dissociated from the plasma were observed as a function of the rf power, and the results are shown in Fig. 4. As the figure shows, an increase in the of rf power increases the optical emission intensities from the dissociated H_α, H_β, Si, and SiH, which appears to suggest an increase in the number of dissociated radicals, such as H, Si, and SiH, at a fixed flow rate of SiH_4 and H_2. In general, the use of high-density plasmas, such as TCP, increases the ion density and the dissociated species in the plasma; an increase in the rf power also increases the ion density and dissociated species. Therefore, the high nano/micro-crystalline silicon percent obtained in this experiment appears related to the high ion density and high number of dissociated species in the plasma used in the experiment.

The change in the crystallinity of the deposited silicon films with increasing rf power was also investigated with

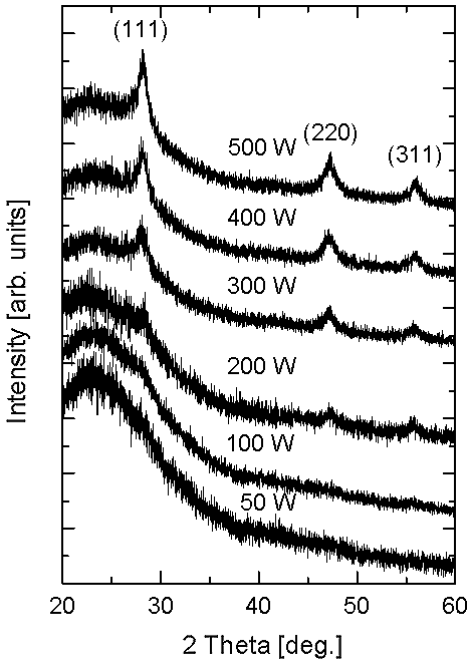

Fig. 5. XRD data of the deposited silicon thin films as a function of the rf power from 50 to 500 W.

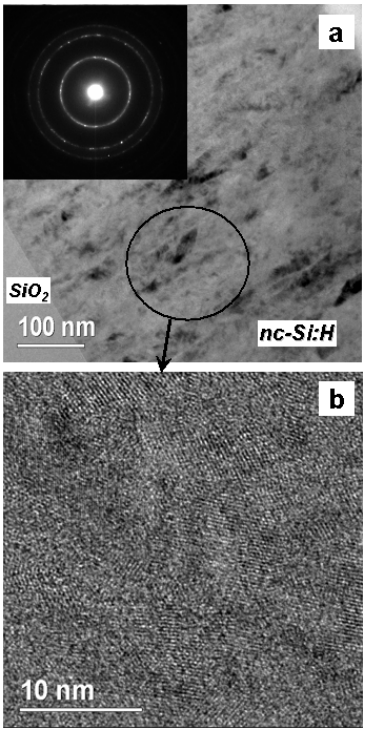

Fig. 6. TEM micrographs and diffraction patterns of the silicon thin film deposited at 500 W.

XRD, and the results are shown in Fig. 5. As the figure shows, the XRD pattern of the films showed peaks related to the (111), the (220), and the (311) crystallographic planes of silicon at 28.18°, 47.26°, and 55.97°, respectively, and the peak intensities increased with increasing rf power, indicating an increase in crystalline percent in the film with increasing rf power. From the peak width of the crystallographic planes, the average grain size of the microcrystalline silicon in the film can be calculated. In general, a wider and broader peak indicates smaller silicon crystallites in the amorphous silicon matrix [21]. Using the following Scherrer formula [22], we calculated the grain size of the crystallites in the film:

$$\Gamma = \frac{k\lambda}{B\cos\theta} \tag{2}$$

where Γ is the grain size, k is the constant 0.9 [22], λ is the wavelength of the X-ray (1.54 Å), B is the full width half maximum (FWHM, radian) of the peaks, and θ is the peak center angle. The grain sizes calculated from Eqs. (2) was in the range from 5.69 to 11.37 nm, and the average grain size was 7.16 nm. The grain size of a crystallite in the film can be also estimated by using the Raman shifts of the peaks in Fig. 2. The suggested formula for calculating the grain size from the Raman shift is [17,23]

$$t = 2\pi(\frac{B}{\Delta\varpi})^{1/2} \tag{3}$$

where t is the calculated grain size, B is the FWHM of the Raman peak from crystalline silicon (about 2.0 cm^{-1} nm^2) [17], and $\Delta\varpi$ is the peak shift for the strained c-Si : H as compared to the peak of the non-strained c-Si : H. The grain size calculated from the Raman shift in Fig. 2 was about 3.12 nm.

The grain size of the nano/micro-crystalline silicon in the film can be observed by using HRTEM. Fig. 6 shows the TEM micrographs of the film deposited on SiO_2 at 500 W. Cross-sectional TEM micrographs and diffraction patterns are shown in the figure. As shown by the cross-sectional TEM micrographs show, the grains were grown with columnar shapes parallel to the growth direction, as described by Bailat *et al.* [24]. In fact, these columnar-shaped grains were composed of merged nanocrystalline grains. When the sizes of the grains in the film was investigated by using HRTEM, as shown in Fig. 6(b), grain sizes ranging from 3 to 15 nm could be identified, and the crystallization percent was around 80 %, similar to the results in Fig. 3 obtained by using Raman spectroscopy. The diffraction pattern obtained from the film also showed the existence of nano-sized crystallites and consisted of three rings from the crystallographic (111), (220), and (311) planes, similar to the XRD data shown in Fig. 5. The thickness of the investigated nano-size crystalline silicon film was about 540 nm. When the nano/micro-crystalline silicon film deposited under the same conditions and having a thickness of about 40 nm was investigated by HRTEM, results similar to those for the 540-nm-thick film were obtained. That is, the increase in the c-Si : H percent obtained in Fig. 3 and 5

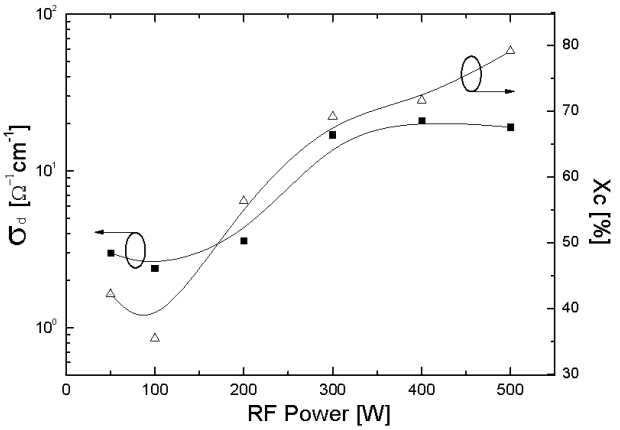

Fig. 7. The dark conductivity (σ_d) of the silicon thin films deposited as a function of the rf power from 50 to 500 W.

might be from an increase in the silicon film's thickness with increasing rf power (from about 100 nm at 50 W to about 540 nm at 500 W) rather than the effect of the rf power itself. However, when the degree of crystallization was observed for the films deposited at the same rf power with different thicknesses (40 nm and 540 nm) by using HRTEM, no significant differences in crystallization could be observed; therefore, it is believed that the increase in the c-Si : H percent obtained in our experiment is more related to the increase in rf power.

The dark conductivity of the 40-nm-thick silicon film as a function of the rf power was measured, and the results are shown in Fig. 7. As the figure shows, with increasing rf power, the conductivity of the film increased, and when the conductivity was compared with the crystallization percent of the film shown in Fig. 3, a similar trend was observed. Therefore, the increase in the conductivity of the film with increasing rf power appears to be related to an increase in the mobility due to an increase in the carrier mean free path caused by the increased crystallization of the film.

IV. CONCLUSIONS

In this study, phosphorous-doped n-type hydrogenated nano/micro-crystalline silicon thin films were fabricated using TCPCVD for applications to solar cells, and the effects of the rf source power on the structural and the electrical properties were investigated. The results showed that with increasing rf power, the crystallization percent of the film increased, possibly due to increased ionization and dissociation of the gas mixture. The increased crystallization with increasing rf power was caused by a decrease in the amount of amorphous silicon and by an increase in the number of strained crystalline silicon grains rather than by an increase in the non-strained large crystalline-silicon grain size. Most of the grain sizes in the film were in the range from 3 to 15 nm; therefore, nano/micro-crystalline silicon grains were formed. The Raman shift with increasing number of nanosized crystalline silicon grains in the film, showed that the stress in the film also increased. The increase in the crystallization percent appears to increase the mobility of the carriers in the film; therefore, the conductivity of the deposited film increased with increasing rf power, a trend similar to the increase in the crystallization percent with increasing rf power. These results were obtained for a 40-nm-thick film, and the structural and the electrical properties of the silicon films obtained in this experiment at 500 W are believed to be applicable to silicon-based solar cells.

ACKNOWLEDGMENTS

This work was supported by the Korean Electronics Technology Institute (KETI), the Nano Information & Energy Storage (NIES) Center, and the National Research Laboratory (NRL) Program of the Korea Ministry of Science and Technology.

REFERENCES

[1] W. E. Spear and P. G. LeComber, Solid State Commun. **17**, 1193 (1975).
[2] C. R. Wronski, D. E. Carlson and R. E. Daniel, Appl. Phys. Lett. **29**, 602 (1976).
[3] C. H. Lee, D. Striakhilev and A. Nathan, J. Vac. Sci Technol. A **22**, 991 (2004).
[4] D. Han, J. D. Lorentzen, J. Weinberg-Wolf, L. E. McNeil and Q. Wang, J. Appl. Phys. **94**, 2930 (2003).
[5] D. Y. Kim, C. K. Sco, M. S. Shim, S. K. Dhungel and J. Yi, J. Korean Phys. Soc. **44**, 1153 (2004).
[6] T. Jana and S. Ray, Thin Solid Films **376**, 241 (2000).
[7] I. Bechers, N. H. Nickel, W. Pilz and W. Fuhs, J. Non-Cryst. Solids **227-230**, 847 (1998).
[8] J. Y. Lee and J. H. Yoon, J. Korean Phys. Soc. **45**, 423 (2004).
[9] A. V. Shah, J. Meier, E. Vallat-Sauvain, N. Wyrsch, U. Kroll, C. Droz and U. Graf, Sol. Energy Mater. Sol. Cells **78**, 469 (2003).
[10] B. Drevillon, I. Solomon and M. Fang, Mater. Res. Soc. Symp. Proc. **283**, 455 (1993).
[11] S. Mukhopadhyay, C. Das and S. Ray, J. Phys. D: Appl. Phys. **37**, 1736 (2004).
[12] S. B. Concari, R. H. Buitrago, M. T. Gutierrez and J. J. Gandia, J. Appl. Phys. **94**, 2417 (2003).
[13] S. Furukawa and T. Miyasato, Phys. Rev. B **38**, 5726 (1988)
[14] S. Veprek, F. A. Sarott and Z. Iqbal, Phys. Rev. B **36**, 3344 (1987).
[15] D. K. Schroder, *Semiconductor Material and Device Characterization* (John Wiley & Sons, New York, 1990), p. 494.

[16] C. Smit, R. A. C. M. M. van Swaaij, H. Donker, A. M. H. N. Petit, W. M. M. Kessels and M. C. M. van de Sanden, J. Appl. Phys. **94**, 3582 (2003).
[17] Y. He, C. Yin, G. Cheng, L. Wang and X. Liu, J. Appl. Phys. **75**, 797 (1994).
[18] A. Matsuda, J. Non-Cryst. Solids **338-340**, 1 (2004).
[19] S. Sriraman, S. Agarwal, E. S. Aydil and D. Maroudas, Nature **418**, 62 (2002).
[20] H. Yang, C. Wu, J. Huang, R. Ding, Y. Zhao, X. Geng and S. Xiong, Thin Solid Films **472**, 125 (2005).
[21] B. D. Cullity, *Elements of X-ray Diffraction*, 2nd edition (Addison-Wesley, Massachusetts, 1978), p. 127.
[22] H. Natter, M. Schmelzer, MS. Loffler, C. E. Krill, A. Fitch and R. Hempelmann, J. Phys. Chem. B **104**, 2467 (2000).
[23] R. Martins, A. Macarico, I. Ferreira, R. Nunes, A. Bicho and E. Fortunato, Thin Solid Films **303**, 47 (1997).
[24] J. Bailat, E. Valllat-Sauvain, L. Feitknecht, C. Droz and A. Shah, J. Appl. Phys. **93**, 5727 (2003).